Biophysical Chemistry, 31 (1988) 163–173
Elsevier

BPC 01297

Determination of cyclopeptide conformations in solution using NMR data and conformational energy calculations

M.D. Shenderovich, G.V. Nikiforovich, J.B. Saulitis and G.I. Chipens

Institute of Organic Synthesis, Latvian S.S.R. Academy of Sciences, Aizkraukles 21, 226006 Riga, U.S.S.R.

Received 5 September 1987
Accepted 1 February 1988

Cyclic peptide; Solution conformation; Energy calculation; Nuclear Overhauser effect

The three-dimensional structure of the cyclic analogs of bradykinin and substance P C-terminal hexapeptide was studied using conformational energy calculations. Initial conformations for energy minimization were selected with the aid of the measured intensities of local nuclear Overhauser effects (NOEs) and other ^{1}H-NMR data. Expected values of the ^{1}H-NMR parameters for low-energy conformations of the cyclopeptides were calculated and compared with those observed experimentally using semiquantitative gradation of NOE intensities. Several low-energy structures of the cyclic bradykinin analog, possessing similar backbone conformations stabilized by two β-turns, are in agreement with experimental data. None of the low-energy conformations of the substance P cyclic hexapeptide were in satisfactory agreement with the experimental set of NOEs. The agreement was achieved only by averaging of the calculated ^{1}H-NMR parameters over several combinations of the low-energy conformations.

1. Introduction

NMR spectroscopy, particularly two-dimensional nuclear Overhauser enhancement (NOE) spectra, is the main source of data on the solution conformations of biomolecules [1]. However, the parameters obtained from NMR spectra provide only fragmentary information on the spatial structure. A more detailed description of the three-dimensional structure of biomolecules can be achieved by theoretical calculations, using the experimental limitations. Distance geometry algorithms [2,3], restrained molecular dynamics [4,5], and conformational energy minimization [6,7] are widely used for this purpose. Of these procedures, energy minimization is the least time-consuming to perform on computers. However, since the molecule is trapped in the local energy minimum nearest to the initial conformation, in the total investigation of spatial structure, minimization should be carried out for many initial conformations. The number of local energy minima under consideration can, however, be substantially reduced by limitations obtained from experimental data. In this paper, we propose a method for determining favorable solution conformations of cyclopeptides, based on energy minimization of conformers selected using ^{1}H-NMR data.

Fig. 1 represents the approach schematically. At the first stage, from the experimental set of NOEs, $^3J_{HNC^{\alpha}H}$ vicinal coupling constants and temperature coefficients $\Delta\delta_{NH}/\Delta T$, those data are

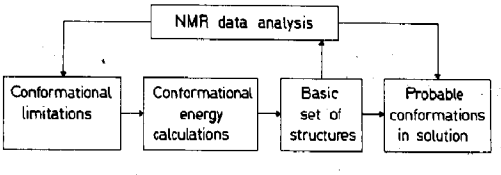

Fig. 1. Schematic representation of the method used for determination of the spatial structure of peptides in solution.

Correspondence address: M. D. Shenderovich, Institute of Organic Synthesis, Latvian S.S.R. Academy of Sciences, Aizkraukles 21, 226006 Riga, U.S.S.R.

selected, which make it possible to limit the number of conformations examined. At the second stage, energy minimization is carried out for initial conformations satisfying the above limitations.

Finally, the basic set of low-energy conformations, thus selected, is compared with the NMR data. The conformers in agreement with experimental data can be regarded as possible models for the spatial structure of peptides in solution. If none of the low-energy conformations presents a satisfactory agreement with the ^{1}H-NMR parameters, conformational averaging of the measured values can be suggested.

The method was applied to investigation of the spatial structure of two cyclic peptides: [cyclo(1 → 9^e),Lys^1,Gly^6]-bradykinin (CBK) with the amino acid sequence [8]

H-Lys^1-Pro^2-Pro^3-Gly^4-Phe^5-Gly^6-Pro^7-Phe^8-Arg^9,

and a cyclic analog of substance P C-terminal hexapeptide (CSP6), with the amino acid sequence [9]

H-Glu^1-Phe^2-Phe^3-Gly^4-Leu^5-Met^6.
└NH(1)-$(CH_2)_3$-NH(2)┘

2. Theory

The intensity ratio for two cross-peaks I_{ij} and I_{kl} in a two-dimensional NOESY spectrum can be expressed through the interproton distances d_{ij} and d_{kl} by eq. 1 [10]:

$$I_{ij}/I_{kl} = \langle d_{ij}^{-6} \rangle / \langle d_{kl}^{-6} \rangle, \quad (1)$$

where the terms $\langle d^{-6} \rangle$ are values averaged over the mixing time τ_m. Eq. 1 is correct, provided that the τ_m value used in experiments corresponds to the linear part of the NOE time dependencies [11], and that the effective correlation times of the interproton vectors are approximately equal [10]. If these conditions are satisfied, an unknown interproton distance can be estimated from eq. 1 using a reference cross-peak corresponding to a known, fixed interproton distance. The farther apart the protons are in the peptide sequence, the more substantial is the limitation of the three-dimensional structure that can be obtained via the distance estimation.

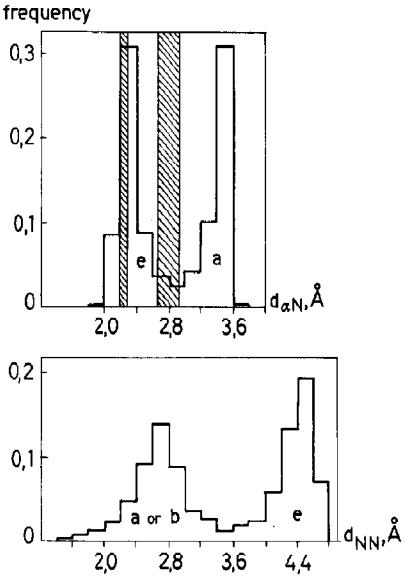

Fig. 2. Distribution of interproton distances $d_{\alpha N}$ and d_{NN} in L-amino acids of 19 proteins, calculated from the data of ref. 14. Theoretical limits for interproton distances $d_{N\alpha}$ are hatched. Letters indicate the corresponding regions of L-amino acid conformations (see fig. 3).

NOEs between protons placed in different parts of a molecule are rarely observed in oligopeptides. However, the NOEs between protons belonging to a single residue or two neighboring residues, used for resonance assignment in ^{1}H-NMR spectra [12], themselves limit the number of possible peptide conformations. The short-range distances $d_{N\alpha}$, $d_{\alpha N}$ and d_{NN} [13] between protons N_iH-$C_i^{\alpha}H$, $C_i^{\alpha}H$-$N_{i+1}H$ and N_iH-$N_{i+1}H$ are determined by the backbone conformation of the i-th amino acid residue [14,15]. NOEs corresponding to these proton pairs will be referred to here as the local NOEs of the given residue and are denoted $NOE_{N\alpha}$, $NOE_{\alpha N}$ and NOE_{NN}.

Frequency diagrams for the occurrence of distances $d_{\alpha N}$ and d_{NN} in L-amino acids of 19 proteins, shown in fig. 2, were calculated on the basis of data presented by Billeter et al. [14]. Theoretical limits on alterations in distance $d_{N\alpha}$ in the permitted conformations of L-amino acid residues are demonstrated in fig. 2 by the hatched

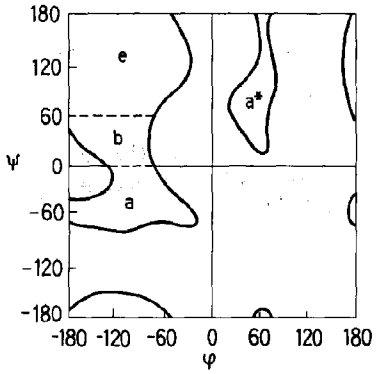

Fig. 3. Main regions of sterically allowed conformations of L-amino acid residues.

bars. First, it should be noted that each of the three interproton distances has two peaks of frequently occurring values, separated by an interval of relatively sparsely populated, intermediate values. The populated ranges of distances $d_{\alpha N}$ and d_{NN} are correlated with the main regions of the conformations allowed for L-amino acid residues (fig. 3). High values of distance d_{NN} ($\gtrsim 4.0$ Å) and low values of distance $d_{\alpha N}$ (2.0–2.5 Å) correspond to the *e* region of extended conformations ($\psi = 120 \pm 60°$). The distribution of these interproton distances expected in the *a* region including the right-handed α-helix conformation, should be the reverse of that in the *e* region. Thus, the *e*- and *a*-type conformers can be differentiated by observed intensities of the $NOE_{\alpha N}$ and NOE_{NN} cross-peaks. Both cross-peaks can have similar intensities in the intermediate *b* region and in the small *a** region, including the left-handed α-helix conformation.

For the majority of L-amino acids, the $d_{N\alpha}$ distance is limited to the narrow interval 2.80 ± 0.15 Å. Lower values (about 2.2 Å) occur only in the *a** region, which is sparsely populated in proteins [16]. Cross-peak intensities, corresponding to these interproton distances, usually cannot fluctuate more than 2-fold in range. Thus, the average intensities of $NOE_{N\alpha}$ cross-peaks can serve as a reference for the estimation of unknown interproton distances or in the prediction of NOE intensities in model conformations. Eq. 1 can be rewritten in this case as

$$I_{ij}/I_{N\alpha} = (d_{N\alpha}/d_{ij})^6, \quad (2)$$

where $I_{N\alpha}$ is the arithmetic mean of all $NOE_{N\alpha}$ intensities, which differ no more than 2-fold, and $d_{N\alpha}$ can be assumed to be equal to 2.8 Å. $NOE_{N\alpha}$ cross-peak intensities can generally be influenced by scalar coupling of the spins [17]. Olejniczak et al. [18] showed, however, that this influence was usually small in pure-phase NOESY spectra.

At the level of approximation of eq. 2 with the accepted mode of cross-peak intensity measurement (see section 3), only semiquantitative estimation of interproton distances, with accuracy no higher than ± 0.5 Å, can be expected [4]. Semiquantitative estimation of NOE cross-peak intensities, instead of interproton distances, is a more suitable means of comparison of suggested models of spatial structure with experimental data. Suzuki et al. [19] proposed the classification of NOEs into grades, with a 2-fold increase in peak intensity between the lower and upper boundaries of the grade. A total difference index was introduced [19] for the comparison of a calculated set of NOEs with observed cross-peak intensities:

$$K = \sum_{i,j} |k_{exp}(i,j) - k_{calc}(i,j)|, \quad (3)$$

where $k_{exp}(i,j)$ and $k_{calc}(i,j)$ are the intensity grade numbers for an observed and calculated NOE, respectively, between protons *i* and *j*. We accepted this approach with the supplementary consideration that two NOEs should be referred to as substantially different only if the difference between corresponding grade numbers exceeds unity.

3. Methods

The synthesis of the cyclopeptides has been described in refs. 8 and 9. All ^{1}H-NMR spectra were obtained in $(C^2H_3)_2SO$ on a Bruker WM-360 spectrometer. Cross-peak intensity in the phase-sensitive NOESY spectra was calculated from the product of the peak height measured in the ω_2 slice and the peak contour area at half height. The mixing times used were 300 ms for CBK and 400

ms for CSP6. Two-dimensional NMR spectra and proton resonance assignment were taken from refs. 21 (CBK) and 22 (CSP6).

Semiempirical energy calculations were carried out, using the peptide geometry and potential functions of Momany et al. [23]. Electrostatic interactions were calculated using the value for the dielectric constant ($\epsilon = 47$) corresponding to $(C^2H_3)_2SO$. Determination of low-energy conformations of cyclopeptides included the following main steps. Firstly, different allowed combinations of amino acid residue standard conformations [24] were generated, and the end-to-end distances in the nonclosed molecules calculated. Preliminary energy minimization, including a weak penalty function to ensure a close arrangement of the backbone terminals, was performed for the initial conformations, with the end-to-end distance being less than the specific limiting value. For the backbone conformations thus selected, the appropriate versions of the precise form assumed on cyclization were determined using the algorithm of Gō and Scheraga [25]. In the final stage, the energy of the whole molecule was minimized over all dihedral angles including the ω angles, the cycle being closed by the set of penalty functions [23].

NOE intensities for the calculated conformations were estimated using eq. 2. $^3J_{HNC^\alpha H}$ vicinal coupling constants were calculated from the Karplus equation using the parameters given by Bystrov et al. [26] and Pardi et al. [27]. As required, the calculated values were averaged over the conformers in the usual way:

$$\langle A \rangle = \sum_i w_i A_i, \tag{4}$$

where $\langle A \rangle$ is the average value of the ^{1}H-NMR parameters, A_i the value calculated for the i-th conformer and w_i the weight of the i-th conformer ($\Sigma_i w_i = 1$).

The low-energy structure or combination of conformers was considered to be in agreement with experimental data if all grade numbers for the calculated and measured NOE intensities (k_{calc} and k_{exp}) satisfied the inequality:

$$|k_{exp} - k_{calc}| \leqslant 1, \tag{5}$$

and provided all $^3J_{HNC^\alpha H}$ vicinal coupling constants, calculated using one of the Karplus curves (ref. 26 or 27) satisfied the condition:

$$|J_{exp} - J_{calc}| \leqslant \Delta J, \tag{6}$$

where the total error ΔJ in the calculated and measured $^3J_{HNC^\alpha H}$ values was assumed to be equal to 1.0, 1.5 or 2.0 Hz.

4. Results and discussion

The diagram in fig 4 demonstrates the distribution of local NOE intensities measured for CBK and CSP6 on an arbitrary scale, common for both peptides. Only αN-type cross-peaks can be observed for prolines and N-terminal residues. For a glycine residue, only NOE_{NN} was considered, since the intensities of other local NOEs are less informative. This is due firstly to the possibility of magnetization transfer between geminal α-protons of glycine [28], and secondly, to the absence of stereospecific resonance assignments for the α-protons.

The measured cross-peak intensities can be divided intuitively into three grades ($k = 1$–3): weak (2–5 intensity units), intermediate (5–8 units) and strong NOEs (> 8 intensity units). This classification was accepted for semiquantitative comparison of calculated and measured NOE intensities with one exception: the lower boundary of the intermediate intensity grade ($k = 2$) was set equal to 4 units. This definition made it possible to differentiate the rather intense NOE_{NN} of Phe^2 in CSP6 from NOE_{NN} of residues Phe^3 and Gly^4, which were not observed at the given signal-to-

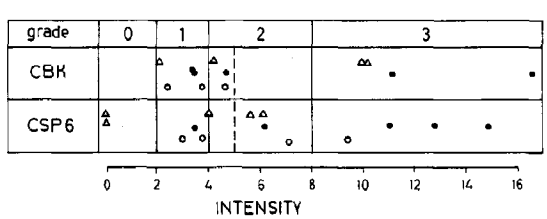

Fig. 4. Distribution of local NOE intensities measured (in arbitrary units) for CBK and CSP6 in $(C^2H_3)_2SO$. (○) $NOE_{N\alpha}$, (●) $NOE_{\alpha N}$, (△) NOE_{NN}.

Table 1

^{1}H-NMR data and conformational limitations for a cyclic analog of bradykinin in $(C^2H_3)_2SO$

Residue	NOE intensity grades			$\Delta\delta_{NH}/\Delta T$ (ppm/K) ($\times 10^3$)	Possible backbone conformations
	Nα	αN	NN		
Pro^3		3			type II
Gly^4			2	3.5	β-bend
Phe^5	1	3	1	2.2	*e*, *b*
Pro^7		1		6.3	type I or III
Phe^8	2	1	3	3.2	β-bend
Arg^9	1	2	3	1.2	*a*, *b*
$N^{\zeta}H$				2.3	

noise ratio ($k = 0$). It should be noted that five out of seven $NOE_{N\alpha}$ cross-peaks observed for both peptides have weak intensities with no more than a 2-fold difference. Similar intensities were measured for several weak αN-type cross-peaks, although they ought to correspond to substantially greater interproton distances ($d_{\alpha N} \simeq 3.5$ Å) according to their distribution in proteins (fig. 2). It can be supposed that the intensity of the weak cross-peaks was increased due to spin diffusion and/or interproton distance fluctuations [29].

5. Cyclic analog of bradykinin

The classification of the NOE intensities and values of the temperature coefficients $\Delta\delta_{NH}/\Delta T$

Table 2

Calculated low-energy conformations of CBK

Parameters		Structure numbers					
		1	2	3	4	5	6
Backbone dihedral angles [a]	ψ_1	91	90	154	155	91	156
	ψ_2	167	165	165	165	161	169
	ψ_3	127	125	138	144	112	139
	φ_4	107	107	90	82	104	87
	ψ_4	−11	−17	3	11	−10	13
	φ_5	−140	−112	−141	−146	−107	−147
	ψ_5	43	50	30	29	80	112
	φ_6	−59	−62	−71	−69	51	−73
	ψ_6	−68	−68	−72	−72	71	−174
	ψ_7	−20	−20	−27	−25	−18	−9
	φ_8	−73	−81	−78	−75	−66	−66
	ψ_8	−65	−36	−32	−34	−27	−25
	φ_9	−98	−162	−162	−163	−70	−151
	ψ_9	−13	92	52	−61	−34	64
$E - E_{min}$ (kcal/mol)		0.0	4.6	6.0	4.9	5.7	7.0
NOE with $\lvert k_{exp} - k_{calc} \rvert > 1$		αN(5) αN(9)	NN(9)	αN(5) NN(5)	αN(5) NN(5) αN(9)	αN(9)	NN(9)
Hydrogen bonds		N_5H- OC_2 N_9H- OC_5 $N_1^{\zeta}H$- OC_6	OC_2 OC_5 –	OC_2 OC_5 –	OC_2 OC_5 OC_5	OC_2 OC_6 OC_7	OC_2 OC_6 –

[a] Values of the dihedral angles ω are usually within the range $180 \pm 15°$.

measured for [cyclo(9 → 1$^{\epsilon}$),Lys^1,Gly^6]-bradykinin in $(C^2H_3)_2SO$, are summarized in table 1. The ^{1}H-NMR data limited the number of possible conformations for all residues excepting Lys^1 and Gly^6 (table 1). Intense NOEs between the δ-protons of prolines in positions 2, 3 and 7, and α-protons of the preceding residues demonstrate unequivocally the *trans* configuration for all X–Pro peptide bonds. The combination of a strong $NOE_{\alpha N}$ for Pro^3, NOE_{NN} for Gly^4 and rather low temperature coefficient for the Phe^5 amide proton suggests [15] the type-II β-bend conformation for the Pro^3-Gly^4 residues. The strong NOE_{NN} of Phe^8 and low temperature coefficient of the Arg^9 amide proton are indications of a second β-bend at Pro^7-Phe^8, that can be assigned from the weak $NOE_{\alpha N}$ of Pro^7 as either a type I or type III bend.

A description of the calculated low-energy conformations for CBK is given in table 2. All of the structures have both postulated β-bends stabilized by hydrogen bonding of the Phe^5 and Arg^9 amide protons. The lysine $N^{\zeta}H$ amide proton, which has a low temperature coefficient $\Delta\delta/\Delta T$, is also hydrogen bonded in some conformations, but the Gly^6 amide proton, with a high $\Delta\delta/\Delta T$, is not involved in any intramolecular hydrogen bond. The $^3J_{HNC^{\alpha}H}$ vicinal coupling constants calculated for structures 1–4 fit the experimental values within an accuracy of 2 Hz. Some coupling constants calculated for structures 5 and 6 deviate from the observed values by more than 3 Hz.

The list of NOEs, showing a substantial difference between the calculated and measured intensities, is given in table 2 for each low-energy

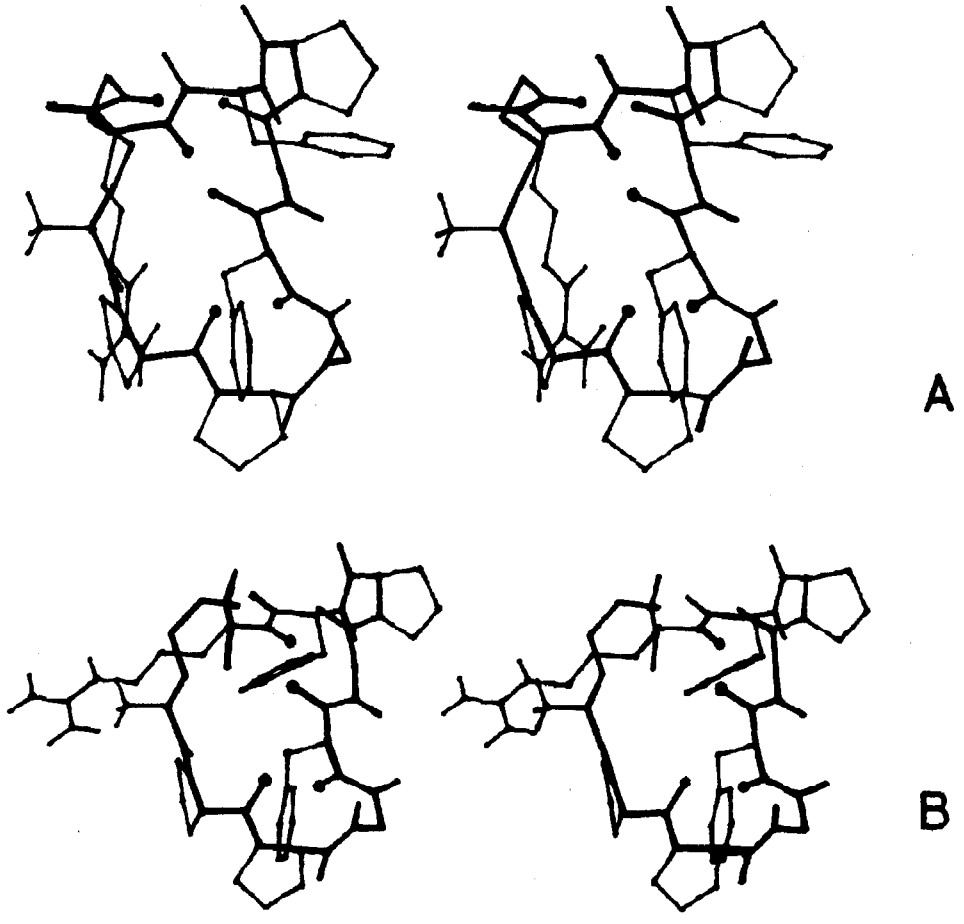

Fig. 5. Stereo drawings of low-energy structures 1 (A) and 2 (B) of CBK.

conformation. All cases of disagreement are related to the NOEs of residues 5 and/or 9. Structures 1–4 have similar backbone conformations for residues 2–8, and differ mainly in terminal residues. Transitions among the possible conformers of C-terminal residues can account for the difference between the calculated and measured NOE intensities of Arg^9. The conformation of Phe^5 in structures 1–4 belongs to the intermediate *b* region, with the interproton distances $d_{\alpha N}$ and d_{NN} being very sensitive to small deviations in the dihedral angles φ and ψ. Conformational fluctuations in this region can result in the $\langle d^{-6} \rangle$ values determining the observed cross-peak intensities, which differ from the $(\langle d \rangle)^{-6}$ values predicted from the static, calculated structures [29].

Stereoviews of low-energy structures 1 and 2 of CBK are given in fig. 5. Both structures are probably typical representatives of the statistical ensemble of cyclopeptide conformers in $(C^2H_3)_2SO$. These structures possess a rigid backbone conformation for residues 2–8, stabilized by two β-bends with intramolecular hydrogen bonds, and a flexible conformation of the C-terminal arginine residue. Such a model for the spatial structure of CBK is in good agreement with available ^{1}H-NMR data. Other versions of the spatial folding of CBK were also predicted by energy calculation. Structures 5 and 6, however, are not in good agreement with the experimental data, and are less preferable than structures 1–4, providing an entropy contribution to free energy is taken into account.

6. Cyclic analog of substance P C-terminal hexapeptide

The distribution of observed NOE intensities (table 3) in $(C^2H_3)_2SO$ does not limit the number of backbone conformations for single residues of CSP6 as substantially as with CBK. Preliminary restriction of the conformations considered for CSP6 was carried out by exclusion of conformers with the expected intensities of separate NOEs exceeding the measured values. Thus, the *a**-type conformers can be excluded when a weak $NOE_{N\alpha}$ is observed (residues 2 and 5), and *e*-type conformers are of low probability with a weak $NOE_{\alpha N}$ (residue 6). The absence of NOE_{NN} restricts the possible conformations of residues 3 and 4 (see table 3). The relatively intense NOE_{NN} for residues 5 and 6, and low temperature coefficients of Met^6 and NH(2) amide protons suggest the possibility of a β-turn conformation in the C-terminal moiety. However, in this case, the type of bend and the exact localization cannot be ascertained without conformational calculations.

More than 40 conformations of CSP6 within an energy limit of 10 kcal/mol were obtained by calculation. Typical representatives of the basic set of structures are described in table 4. The expected intensities of local NOEs were calculated for each structure. None of the basic structures show satisfactory agreement with the experimental set of NOEs. Each low-energy conformation predicts substantial differences between the calcu-

Table 3

^{1}H-NMR data and conformational limitations for a cyclic analog of substance P C-terminal hexapeptide in $(C^2H_3)_2SO$

Residue	NOE intensity grades			$\Delta\delta_{NH}/\Delta T$ (ppm/K) ($\times 10^3$)	Possible backbone conformations [a]
	Nα	αN	NN		
Glu^1		3			*e*
Phe^2	1	3	2	1.3	*e* and *a*, *b*
Phe^3	3	3	0	4.8	*e* and *a**
Gly^4			0	4.3	*e* or *e**
Leu^5	1	2	2	4.3	*e* and *a*, *b*
Met^6	2	1	2	1.3	*a* or *a**
NH(2)				0.7	

[a] Local NOE intensities for residues 2, 3 and 5 can be explained by averaging over conformers from the different regions (and); data observed for residues 4 and 6 can be explained by conformers from any of the given regions (or).

Table 4

Representative low-energy structures of CSP6

Parameters		Cluster numbers							
		1	2	3	4	5	6	7	8
Backbone dihedral angles [a]	ψ_1	138	120	131	116	115	137	152	113
	φ_2	−145	−151	−146	−96	−86	−82	−81	−82
	ψ_2	164	61	63	175	−35	−24	−26	−25
	φ_3	−78	−140	51	54	−140	−151	49	54
	ψ_3	126	64	37	39	152	158	63	40
	φ_4	165	173	−89	64	−71	−79	−172	176
	ψ_4	−178	−168	158	−166	76	69	−136	−68
	φ_5	−73	−64	−74	−64	−97	−87	−66	−81
	ψ_5	−47	107	−51	148	−59	83	−44	89
	φ_6	−79	51	−83	59	−95	53	−71	52
	ψ_6	−36	42	−36	69	−41	43	−35	47
$E - E_{min}$ (kcal/mol)		0.0	5.4	4.0	4.6	1.5	4.2	4.8	4.8
NOE with $\lvert k_{exp} - k_{calc} \rvert > 1$		NN(2) Nα(3) αN(5)	Nα(3) NN(5)	αN(3) αN(5)	NN(2) αN(3) NN(5)	αN(2) Nα(3) αN(5)	αN(2) Nα(3) NN(5)	αN(2) αN(5)	αN(2) αN(3) NN(5)
Accessible surface area of amide protons [b] (Å^2)		N_2H 0.0	0.0	1.1	0.0	1.3	1.8	0.0	0.0
		N_3H 4.9	0.0	1.8	8.4	1.3	1.3	0.0	0.0
		N_4H 2.1	2.2	0.0	7.5	5.6	4.5	0.0	0.0
		N_5H 8.0	8.4	7.7	8.6	0.0	0.0	7.0	0.0
		N_6H 2.1	6.3	2.6	2.3	0.1	3.9	1.8	3.8
		NH(2) 0.0	1.4	2.0	0.5	0.0	3.2	0.0	2.0

[a] Values of the dihedral angles ω are usually within the range $180 \pm 10°$.

[b] Calculated according to the method of Lee and Richards [31].

lated and observed intensities for at least two local NOEs. This discrepancy is involved mainly with the effects of residues 2, 3 and 5.

As mentioned in section 2, one intense NOE corresponds to each of three main, allowable conformational regions for L-amino acid residues (fig. 3). Nevertheless, two rather intense effects were observed for most CSP6 residues. This is possible

Table 5

Results of ^{1}H-NMR parameter averaging over the different combinations of CSP6 low-energy structures

Combinations [a] of clusters	ΔJ (Hz) [b]	K_{min} [c]	Weight limits (×100) [d]		
			w_1	w_2	w_3
4,5	1.5	5	59–76	24–41	
3,6	2.0	5	65–77	23–35	
1,4,5	1.0	2	16–47	13–50	32–43
3,4,5	1.0	3	15–26	38–54	30–38
2,3,5	1.0	4	18–44	25–57	22–32
1,3,6	1.5	4	4–52	11–71	13–46

[a] ^{1}H-NMR parameters were averaged over the representative structures of the clusters (see table 4).

[b] Minimum of the three values $\Delta J = 1.0$, 1.5 and 2.0 Hz for which all conditions (eq. 6) are satisfied.

[c] Minimum value of the total difference index; see eq. 3.

[d] Minimum and maximum weights of the corresponding structures, obtained with the given values of ΔJ and K_{min}.

in the case of either a very specific spatial structure or equilibrium between essentially different structures. The fact that none of more than 40 low-energy conformations can completely satisfy the experimental data suggests, in our opinion, that conformational equilibrium is the most probable explanation for the observed cross-peak intensities.

With the basic set of structures, we attempted to select the combinations of conformers giving calculated average values in agreement with observed NOEs and other ^{1}H-NMR parameters. This analysis was feasible for a limited number of structure combinations. Therefore, calculated structures predicting similar intensities for all NOEs under investigation were united into clusters. Table 4 lists eight clusters of structures selected according to this criterion with four types of Phe^2-Phe^3 conformers (*ee*, *ea**, *ae* and *aa**) and two types of Leu^5-Met^6 conformers (*aa* and *ea**). Clusters 7 and 8 each contain single conformations, while other clusters include from 4 to 10 low-energy conformations. A single representative structure was selected for averaging from each cluster (energies are given in table 4).

Double and triple combinations of representative structures, with expected agreement between the measured and calculated average ^{1}H-NMR parameters, were selected by preliminary analysis. Random sets of weights w_i were generated for these combinations of structures. The average intensities of 14 NOEs and average values of six $^3J_{HNC^{\alpha}H}$ coupling constants were calculated for each set of weights. Results for the combinations giving the best agreement between calculated and observed values are listed in table 5. A satisfactory agreement can be achieved by averaging over the pairs of structures from clusters 4,5 or 3,6, but the best agreement was obtained in the combinations of structures from clusters 1,4 and 5 or 3,4 and 5. However, in both combinations, the average intensity of the Phe^2 $NOE_{\alpha N}$ remains at only about half of the value measured. An attempt to achieve better agreement for this NOE, by adding a fourth structure from clusters 2 or 3, was unsuccessful. It should be borne in mind, however, that cross-peaks corresponding to the amide proton of Phe^2 and the α-protons of Phe^2 and Phe^3 overlap in the NOESY spectrum of CSP6, and that the accepted method of measurement can overestimate the intensities of these cross-peaks.

The conformations possible for the CSP6 molecule are represented in fig. 6 by stereoviews of three structures from clusters 1, 4 and 5. It should be noted that these conformations differ in both main chain folding and orientation of the side chains, which are mainly directed toward the solvent. The C-terminal moiety of the molecule usually forms a β-bend with corner residues Leu^5-Met^6. This can be either a type II bend stabilized by a $4 \rightarrow 1$ hydrogen bond or a type III bend without a hydrogen bond. In some structures (not shown in fig. 6), the Leu^5 residue forms a γ-turn stabilized by a $3 \rightarrow 1$ hydrogen bond. The carbonyl group of the glutamic acid side chain can form hydrogen bonds with the amide groups of different residues.

According to the $\Delta\delta_{NH}/\Delta T$ values [30] measured in $(C^2H_3)_2SO$ (table 3), the amide protons of CSP6 can be divided into two groups; the protons of Phe^2, Met^6 and NH(2), which should, to a considerable extent, be screened from solvent and the amide protons of residues 3–5 which would be expected to be exposed to solvent. The accessible surface areas of the amide protons in the low-energy structures of CSP6, shown in table 4, were calculated by the method of Lee and Richards [31], using the van der Waals radii given by Bondi [32] and a probe radius of 1.4 Å, corresponding to a water molecule. Naturally, these values can be compared with experimental data obtained in $(C^2H_3)_2SO$ only with reservation, but at any rate, the amide protons barely accessible to H_2O molecules should be even more screened from the bulky molecules of $(C^2H_3)_2SO$.

In most of the structures set out in table 4, the amide protons of Phe^2, Met^6 and NH(2) are completely, or to a considerable extent, screened from solvent. The accessible area for amide protons 3–5 is substantially different from one structure to another. However, in the conformational equilibria of structures from clusters 1,4 and 5 or 3,4 and 5, each of these amide protons should be partly exposed to solvent. Thus, the assumption on the conformational equilibrium of several low-energy structures of CSP6 is also in qualitative

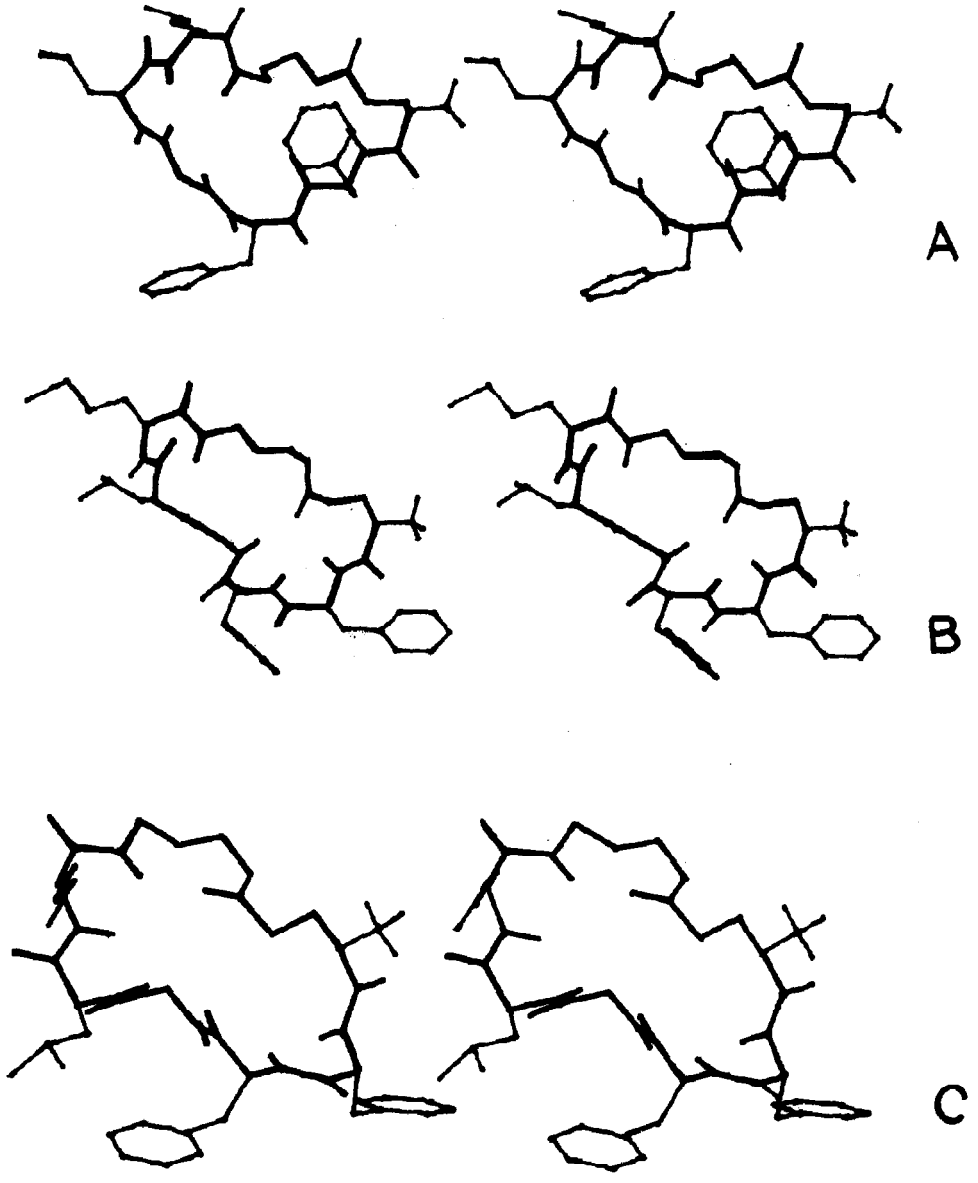

Fig. 6. Stereo drawings of the representative low-energy conformations of CSP6 from clusters 1 (A), 4 (B) and 5 (C).

agreement with the temperature dependencies of the amide proton chemical shifts in $(C^2H_3)_2SO$.

Certainly, the method applied to the calculation and averaging of NMR parameters is a rather rough approximation. Using this procedure, we cannot hope to obtain a real description of the conformational dynamics for CSP6. The results of this investigation prove only that the dynamic equilibrium of conformers accounts for the available experimental data far better than each selected low-energy structure. Moreover, the conformer combinations, in the case where the averaged values of the NMR parameters do not contradict the experimental data, can serve as a first approximation in a more detailed study of the conformational properties of a cyclopeptide by Monte Carlo

[33,34] or molecular dynamics [2,3] simulation.

7. Conclusions

The results presented here relate to two small peptides, of which the conformational mobility is restricted by cyclization. Nevertheless, the CSP6 molecule proves to be conformationally flexible in solution. CBK has a rather rigid spatial structure in dimethyl sulfoxide. In this case, however, the more flexible part of the main chain was also selected. Dynamic equilibrium in solution, with conformational transitions of molecular fragments, or even entire molecules, is probably a common property of oligopeptides. Therefore, static models do not give a complete representation of the three-dimensional structure of oligopeptides. A complete description of the spatial structure can be obtained only in the form of a statistical ensemble of conformers.

References

1 A.E. Derome, Modern NMR techniques for chemistry research (Pergamon Press, Oxford, 1987).
2 T.F. Havel and K. Wüthrich, Bull. Math. Biol. 46 (1984) 673.
3 M.P. Williamson, T.F. Havel and K. Wüthrich, J. Mol. Biol. 182 (1985) 295.
4 G.M. Clore, A.M. Gronenborn, A.T. Brünger and M. Karplus, J. Mol. Biol. 186 (1985) 435.
5 G.M. Clore, A.M. Gronenborn, G. Carlson and E.F. Meyer, J. Mol. Biol. 190 (1986) 259.
6 A.S. Arseniev, I.L. Barsukov, V.F. Bystrov, A.L. Lomize and Yu.A. Ovchinnikov, FEBS Lett. 186 (1985) 168.
7 M.D. Shenderovich, I.P. Sekacis, E.E. Liepinsh, G.V. Nikiforovich and O.S. Papsuevich, Bioorg. Khim. 11 (1985) 1180.
8 G. Chipens, F. Mutulis and S. Galaktionov, in: Frontiers of bioorganic chemistry and molecular biology, ed. S.N. Anancenko (Pergamon Press, New York, 1980) p. 99.
9 F.K. Mutulis, I.E. Mutule, G.H. Maurops, I.P. Sekacis, V.D. Grigoryeva, E.M. Kukaine, V.V. Golubeva, N.V. Myshlyakova, V.E. Klusha and G.I. Chipens, Bioorg. Khim. 11 (1985) 1276.
10 G.M. Clore and A.M. Gronenborn, J. Magn. Reson. 61 (1985) 158.
11 C.M. Dobson, E.T. Oleyniczak, F.M. Poulsen and R.G. Ratcliffe, J. Magn. Reson. 48 (1982) 97.
12 G. Wagner, A. Kumar and K. Wüthrich, Eur. J. Biochem. 114 (1981) 375.
13 K. Wüthrich, M. Billeter and W. Braun, J. Mol. Biol. 180 (1984) 715.
14 M. Billeter, W. Braun and K. Wüthrich, J. Mol. Biol. 155 (1982) 321.
15 M.D. Shenderovich, G.V. Nikiforovich and G.I. Chipens, J. Magn. Reson. 59 (1984) 1.
16 J.S. Richardson, Adv. Protein Chem. 34 (1981) 167.
17 S. Macura, Y. Huang, D. Suter and R.R. Ernst, J. Magn. Reson. 43 (1981) 259.
18 E.T. Olejniczak, J.C. Hoch, C.M. Dobson and F.M. Poulsen, J. Magn. Reson. 64 (1985) 199.
19 E. Suzuki, N. Pattabiraman, G. Zon and T.L. James, Biochemistry 25 (1986) 6854.
20 G. Chipens, F. Mutulis, B. Katayev, V. Klusha, I. Misina and N. Myshlyakova, Int. J. Peptide Protein Res. 18 (1981) 302.
21 J. Saulitis, B. Liepins, I. Sekacis, M. Shenderovich, F. Mutulis, I. Mutule and G. Chipens, Bioorg. Khim. 11 (1985) 1013.
22 J. Saulitis and E. Liepins, Bioorg. Khim. 13 (1987) 168.
23 F.A. Momany, R.F. McGuire, A.W. Burgess and H.A. Scheraga, J. Phys. Chem. 79 (1975) 2361.
24 S.S. Zimmerman and H.A. Scheraga, Biopolymers 16 (1977) 811.
25 N. Gō and H.A. Scheraga, Macromolecules 3 (1970) 178.
26 V.F. Bystrov, V.T. Ivanov, S.L. Portnova, T.A. Balashova and Yu.A. Ovchinnikov, Tetrahedron 29 (1973) 873.
27 A. Pardi, M. Billeter and K. Wüthrich, J. Mol. Biol. 180 (1984) 741.
28 L.E. Kay, T.A. Holak, B.A. Johnson, I.M. Armitage and J.H. Prestegard, J. Am. Chem. Soc. 108 (1986) 4242.
29 G.M. Clore, A.M. Gronenborn and W. McLaughlin, Eur. J. Biochem. 151 (1985) 153.
30 A. Bundi, C. Grathwohl, J. Hochmann, R.M. Keller, G. Wagner and K. Wüthrich, J. Magn. Reson. 18 (1975) 191.
31 B. Lee and F.M. Richards, J. Mol. Biol. 55 (1971) 379.
32 A. Bondi, J. Phys. Chem. 68 (1964) 441.
33 G.H. Paine and H.A. Scheraga, Biopolymers 24 (1985) 1391.
34 J. Betins, G.V. Nikiforovich and G. Chipens, J. Mol. Struct. 137 (1986) 129.